Dynamic Properties of Monolithic 1.3 μm InAs/GaAs Quantum Dot Lasers on Silicon

Constanze Hantschmann[1], Peter P. Vasil'ev[1,3], Siming M. Chen[2], Mengya Liao[2], Alwyn J. Seeds[2], Huiyun Liu[2], Richard V. Penty[1], and Ian H. White[1]

[1]*Centre for Photonic Systems, Department of Engineering, University of Cambridge, 9 JJ Thomson Avenue, Cambridge CB3 0FA, UK*
cb893@cam.ac.uk

[2]*Department of Electronic and Electrical Engineering, University College London, Torrington Place, London WC1E 7JE, UK*

[3]*Also associated with the PN Lebedev Physical Institute, 53 Leninsky Prospect, Moscow 119991, Russia*

Abstract: Small-signal experiments with a 2.5 mm-long quantum dot narrow ridge-waveguide laser on silicon show a modulation bandwidth of 1.6 GHz. For the first time, we report key high-speed parameters such as the differential gain and the gain compression factor for the respective quantum dot laser.

1. Introduction

The demonstration of InAs/GaAs quantum dot (QD) lasers monolithically grown on silicon (Si) substrate operating continuous-wave (cw) at room and elevated temperatures has been a major milestone towards photonic integrated circuits. Devices with low threshold currents, high efficiency, high output powers, and long lifetimes have demonstrated an excellent static performance [1], whereas recently measured 3dB bandwidths of 4 GHz and 6.5 GHz for devices with an undoped and a *p*-doped active region indicate that QD lasers on Si are attractive candidates for optical communications as well [2]. In this paper, we present the small-signal modulation of a 2.5 mm-long QD narrow ridge-waveguide laser with an undoped active region on Si substrate. By using simple analytical equations, we gain an intuitive insight into the underlying physics and report, to the best of our knowledge, the first ever values of the differential gain and the gain compression factor of a Si-based QD laser.

2. Theoretical background

The small-signal modulation response of a semiconductor laser diode is typically analyzed using the standard three-pole transfer function based on a two-pole function with the resonance frequency f_R and the damping γ as fitting parameters, and an additional pole to account for electrical parasitics [2]. f_R and γ are linked by the *K*-factor and the damping offset γ_0 as $\gamma = Kf_R^2 + \gamma_0$, and further definitions of f_R and the *K*-factor are given by

$$f_R^2 = \frac{1}{4\pi^2}\frac{v_{gr}\,{}^{\partial g}/_{\partial N}S}{\tau_{ph}} = \frac{1}{4\pi^2}\frac{v_{gr}\eta\Gamma\,{}^{\partial g}/_{\partial N}}{eV_{Dots}} \cdot (I - I_{th}) \tag{1}$$

$$K = 4\pi^2\tau_{ph}\left(1 + \frac{\Gamma\,{}^{\partial g}/_{\partial S}}{{}^{\partial g}/_{\partial N}}\right) . \tag{2}$$

In (1), v_{gr}, $\partial g/\partial N$, S, τ_{ph}, η, Γ, e, V_{Dots}, and I-I_{th} are the group velocity, the differential gain, the photon density, the photon lifetime, the injection efficiency, the confinement factor, the elementary charge, the QD volume, and the current above threshold, and in (2), $\partial g/\partial S$ is the gain derivative with respect to S [3].

3. Device structure and static properties

First, various buffer and dislocation filter layers are grown under carefully adjusted growth conditions on the intentionally miscut Si substrate as explained in [4]. The actual InAs/GaAs QD laser comprises an undoped five-layer InAs/InGaAs/GaAs dot-in-a-well stack in a GaAs waveguide, which is sandwiched between an *n*-doped cladding and a p/p^+-doped cladding and contact layer. Narrow ridge-waveguide lasers with dimensions of 2.2 μm × 2.5 mm and a high-reflection coating at the rear facet are then fabricated and finally mounted on a copper heatsink. At room temperature with the heatsink set to 15 °C, a threshold of 20 mA and a slope of about 0.09 W/A are obtained from the laser's cw LI curve. The laser oscillates at 1310 nm in single-transverse but multi-longitudinal mode operation.

4. Small-signal modulation and analysis

The modulation response curves of the Si-based QD laser can be seen in Fig. 1(a), demonstrating a maximum bandwidth of 1.6 GHz. As shown in the inset, the linear fit of the first three data points of f_{3dB} versus $(I\text{-}I_{th})^{1/2}$ gives a modulation current efficiency of 0.4 GHz/mA$^{1/2}$. The sublinear trend at higher currents indicates the onset of strong

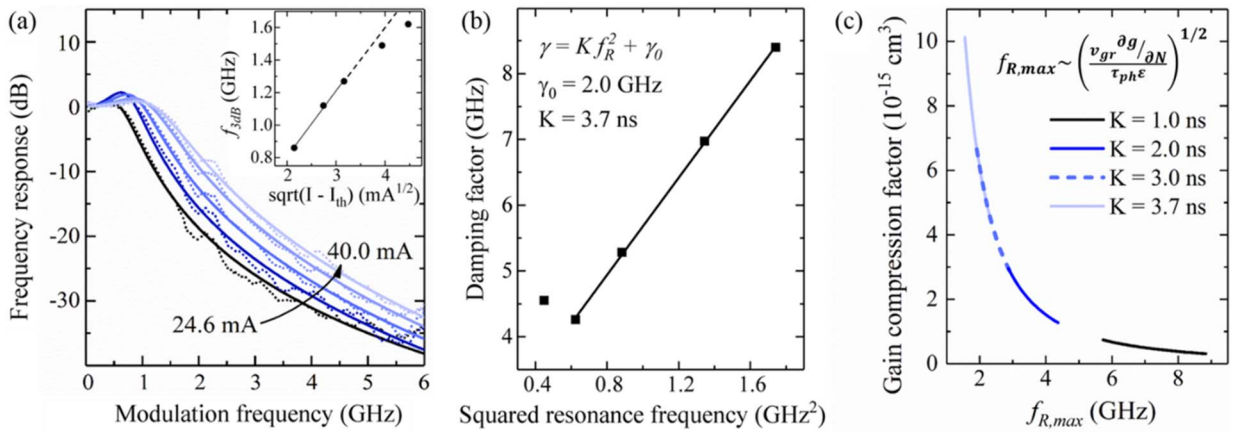

Fig. 1. (a) Smoothed and normalized small-signal modulation response curves of the QD laser on Si recorded at different currents. The inset shows the 3dB frequency versus the square root of the current above threshold. (b) Linearly fitted damping versus the squared resonance frequency. (c) Gain compression factor plotted against the maximum resonance frequency calculated for different *K*-factors.

damping effects. Using the three-pole transfer function, the bias-dependent resonance frequencies and damping values are extracted and plotted as shown in Fig. 1(b). From the linear fit, a damping offset of $\gamma_0 = 2.0$ GHz, corresponding to an effective carrier lifetime of $\tau \approx \gamma_0^{-1} = 0.5$ ns, and a large *K*-factor of 3.7 ns are obtained. Compared with the bandwidth of 4 GHz and the *K*-factor of 1.3 ns reported for the undoped laser in [2], a major reason for our lower modulation bandwidth and higher K-factor is the long laser cavity and hence long photon lifetime. For the tested 2.5 mm-long laser, τ_{ph} is about twice that of the 580 µm-short laser used in [2], which translates directly into a reduced resonance frequency and a higher *K*-factor, as can be seen from Eqs. (1) and (2). Based on (2), the remaining difference suggests that reducing gain compression effects and increasing the differential gain, for instance by *p*-modulation doping, can help achieving higher modulation bandwidths.

The differential gain is estimated using Eq. (1), assuming $\Gamma = 5 \times 10^{-4}$. This yields a value of approximately 2×10^{-15} cm^2, which is well comparable with values for InAs QD lasers on their native substrate [5,6]. By deriving $\partial g/\partial S$ from (2) and using the relationship between $\partial g/\partial S$ and the gain compression factor ε [3], we obtain $\varepsilon \approx 0.5\text{-}1.5 \times 10^{-15}$ cm^3. Since this calculation neglects the impact of carrier transport effects, it is compared to an approach assuming $f_{R,max} \sim 1/\sqrt{\varepsilon}$ at high output powers [3]. Assuming that the upper boundary for the maximum resonance frequency is given by $f_{3dB,max} = 2\pi\sqrt{2}/K$, Fig. 1(c) plots ε against $f_{R,max}$. It can be seen that for $K = 1$ ns, a gain compression factor of about 10^{-16} cm^3 is derived, which is a common value for QD lasers on GaAs [6]. For higher *K*-factors, values around 10^{-15} cm^3 and higher are reached, hence confirming the previous result.

5. Conclusion

In conclusion, we have reported small-signal modulation experiments with a 2.5 mm-long narrow ridge-waveguide 1.3 µm InAs/GaAs QD laser directly grown Si with a 3dB bandwidth of 1.6 GHz. By analyzing the modulation response curves with a three-pole transfer function, an effective carrier lifetime of 0.5 ns and a *K*-factor of 3.7 ns were extracted. In addition, we have calculated the first ever values of the differential gain and the gain compression factor for a Si-based QD laser, obtaining a differential gain of about 2×10^{-15} cm^2 and a high gain compression factor on the order of 10^{-15} cm^3. Whereas these results indicate that the tested devices have the potential for data transmission applications if designed accordingly, they also highlight that much remains to be learnt about their intrinsic physics.

6. References

[1] J. C. Norman, D. Jung, Y. Wan, and J. E. Bowers, "Perspective: The future of quantum dot photonic integrated circuits," APL Photon., Vol. 3, pp. 030901, Mar. 2018.

[2] D. Inoue, D. Jung, J. Norman, Y. Wan, N. Nishiyama, S. Arai et al., "Directly modulated 1.3 µm quantum dot lasers epitaxially grown on silicon," Opt. Express, Vol. 26, no. 6, pp. 7022-7033, Mar. 2018.

[3] L. A. Coldren and S. W. Corzine, *Diode lasers and photonic integrated circuits* (John Wiley & Sons, 1995), Chap. 5.

[4] S. Chen, W. Li, J. Wu, Q. Jiang, M. Tang, S. Shutts et al., "Electrically pumped continuous-wave III-V quantum dot lasers on silicon," Nat. Photonics, Vol. 10, no. 5, pp. 307-311, Mar. 2016.

[5] M. Kuntz, G. Fiol, M. Lämmlin, D. Bimberg, M. G. Thompson, K. T. Tan et al., "Direct modulation and mode locking of 1.3 µm quantum dot lasers," New J. Phys., Vol. 6, no. 1, pp. 181, Nov. 2004.

[6] S. Fathpour, Z. Mi, and P. Bhattacharya, "High-speed quantum dot lasers," J. Phys. D: Appl. Phys., Vol. 38, no. 13, pp. 2103-2111, June 2005.